Functional Decoupling of BOLD and Gamma-Band Amplitudes in Human Primary Visual Cortex

Suresh D. Muthukumaraswamy* and Krish D. Singh

Cardiff University Brain Research Imaging Centre (CUBRIC), School of Psychology, Cardiff University, Cardiff CF10 3AT, United Kingdom

Abstract: Although functional magnetic resonance imaging is an important tool for measuring brain activity, the hemodynamic blood oxygenation level dependent (BOLD) response is only an indirect measure of neuronal activity. Converging evidence obtained from simultaneous recording of hemodynamic and electrical measures suggest that the best correlate of the BOLD response in primary visual cortex is gamma-band oscillations (~40 Hz). Here, we examined the coupling between BOLD and gamma-band amplitudes measured with magntoencephalography (MEG) in human primary visual cortex in 10 participants. In Experiment A, participants were exposed to grating stimuli at two contrast levels and two spatial frequencies and in Experiment B square and sine wave stimuli at two spatial frequencies. The amplitudes of both gamma-band oscillations and BOLD showed tuning with stimulus contrast and stimulus type; however, gamma-band oscillations showed a 300% increase across two spatial frequencies, whereas BOLD exhibited no change. This functional decoupling demonstrates that increased amplitude of gamma-band oscillations as measured with MEG is not sufficient to drive the subsequent BOLD response. *Hum Brain Mapp 30:2000–2007, 2009.* © 2008 Wiley-Liss, Inc.

Key words: oscillations; magnetoencephalography; functional magnetic resonance imaging; spatial frequency; V1

INTRODUCTION

Functional magnetic resonance imaging (fMRI) measuring the blood oxygenation level dependent (BOLD) response is one of the most popular tools for characterising brain activity in human neuroscience. However, this hemodynamic signal is only an indirect measure of neuronal activity. Invasive simultaneous recording work in animals [Logothetis et al., 2001] has demonstrated a complex origin of the BOLD response, which appears correlated not only to local field potentials but also to some extent in multiunit activity. Similar findings have also been reported when BOLD and invasive recordings are made non-simultaneously [Kayser et al., 2004; Nir et al., 2007]. A recent experiment [Niessing et al., 2005] has demonstrated that the amplitude of hemodynamic signals as measured with optical imaging in cats can be tightly localised with gamma-band activity both spatially and functionally, with the amplitude of both hemodynamic and gamma-band local field potentials increasing in a similar fashion with stimulus contrast. Fluctuations of the BOLD response to the same stimulus correlate well with corresponding fluctuations in the gamma-band response [Niessing et al., 2005]. Similarly, in an experiment stimulating cat visual cortex with simple and complex natural stimuli the best match between BOLD and local field potentials was found in the gamma frequency range [Kayser et al., 2004]. Convergent evidence

Additional Supporting Information may be found in the online version of this article.

Contract grant sponsor: Biotechnology and Biological Sciences Research Council (BBSRC); Contract grant number: BBS/B/08035.

*Correspondence to: Suresh Muthukumaraswamy, School of Psychology, Cardiff University, CUBRIC Building, Park Place, Cardiff, CF10 3AT. E-mail: sdmuthu@cardiff.ac.uk

Received for publication 16 April 2008; Revised 3 June 2008; Accepted 29 June 2008

DOI: 10.1002/hbm.20644

Published online 26 August 2008 in Wiley InterScience (www.interscience.wiley.com).

therefore suggests that in primary visual cortex gamma-band oscillations are perhaps the closest neural signature to the BOLD response yet found and the simple hypothesis presents itself that gamma-band oscillations may be the main neural response causing the subsequent BOLD response in primary visual cortex.

To examine the relationship between gamma-band activity and the BOLD response, we recorded dense-array (275-channel) magntoencephalography (MEG) to quantify gamma-band activity and measured the BOLD response with fMRI. Although separate recording sessions were used for each modality the same 10 participants were recorded from and were exposed to identical stimulus parameters and protocols. With the growth of MEG and EEG as neuroimaging techniques that directly measure neuronal activity, it is important to understand the physiological relationship between BOLD and the dependent variables that these techniques measure as well as how invasive measures correlate to BOLD. Although simultaneous recording of EEG-fMRI is now possible, it invariably incurs a significant reduction in both signal to noise [Parkes et al., 2006] and spatial sampling (number of channels recorded) such that it is most useful where single trial data are to be directly compared between the recording modalities or in paradigms where the functional system of interest is likely to change between recording sessions (for example, in learning paradigms).

In a previous experiment where we applied this joint MEG/fMRI methodology, we compared spatiotemporal frequency tuning between gamma-band responses and the BOLD signal [Muthukumaraswamy and Singh, 2008] and noted a large discrepancy between the responses with respect to spatial frequency. Specifically, we found in primary visual cortex that gamma-band amplitudes were three times larger for a 0.5 cycles per degree (cpd) stimulus compared to a 3 cpd stimulus. However, the BOLD response showed a similar amplitude level for both stimuli. This result suggested that BOLD and gamma-band amplitudes can be functionally decoupled; a result that would imply, at least for primary visual cortex, that increased amplitude of gamma-band oscillations is not sufficient to drive the subsequent BOLD response. However, several factors limited such an interpretation of these previous data. First, because only maximal contrast stimuli were used in the experiment, the flat BOLD response between the two stimuli may have been either a ceiling effect in the BOLD response or a contrast saturation effect. To address this issue here, in Experiment A, we used both maximal contrast (100%) and a lower contrast level (30%). A second issue with interpreting our previous experiment [Muthukumaraswamy and Singh, 2008] was that only square wave grating stimuli were used, which contain harmonic spatial frequencies. For example, a 0.5 cpd square wave stimulus will contain a first harmonic at 1.5 cpd and a second harmonic at 2.5 cpd (odd integer multiples of the fundamental frequency). If the BOLD response was differentially sensitive to these spatial frequencies, this may have elevated the BOLD response. To address this here, in Experiment B, participants were stimulated with sine and square-wave grating stimuli at the same two spatial frequencies.

MATERIALS AND METHODS

Participants, Stimuli, and Paradigm

Ten healthy right-handed volunteers with normal or corrected to normal vision including eight females and two males (mean age 27; range 23–30) participated in the experiment after giving informed consent. All procedures were approved by the local Ethics Committee. One participant performed the MEG component twice because of poor data quality (head movement) in the first recording. Only data from the second recording session of this participant are included here.

Identical participants, stimuli, and paradigm-design were used for both the MEG and fMRI sessions. This consisted of vertical stationary gratings (0 Hz temporal frequency) presented using Presentation software (Neurobehavioral Systems) on a mean luminance background. In Experiment A, square wave grating stimuli were presented at two spatial frequencies (3 and 0.5 cpd) each at two different contrast levels (30 and 100%). Thirty percent stimulus contrast was used as the lower contrast as it still allowed relatively good signal to noise in both our dependent variables. In Experiment B, two different spatial frequencies were presented (3 and 0.5 cpd) as either square or sine wave gratings (contrast level 100%). The video-card drove both projection systems at 60 Hz refresh rate at 1024×768 pixel resolution. For the MEG, a Sanyo XP41 LCD back-projection system was used and for the MRI a Canon Xeed SX60 projector. Each set of stimuli (fMRI/MEG) was gamma corrected for the projector used to account for possible differences in the two projection systems. Stimuli were presented in the lower left visual field with the upper right corner of the stimulus located 1° horizontally and vertically from a small fixation cross. Stimuli subtended 8° both horizontally and vertically. Participants were instructed to maintain fixation for the entire experiment, and in order to maintain attention they were instructed to press a response key at the termination of each stimulation period. Five hundred millisecond offset jitter was added to each stimulus duration.

On separate days, each participant underwent fMRI or MEG scanning consisting of four runs each lasting 10 min back to back. Participants performed either two runs of Experiment A or two runs of Experiment B first. Run and scanning order was counterbalanced across participants. A run consisted of 40 trials in a 15-s boxcar design with a 10 s rest period followed by a 5 s active stimulation period. The four different stimuli used in each experiment were presented in pseudo-randomised fashion in each of the runs (each stimulus type was presented 10 times in each of two runs making a total duration of 100 s). Our

temporal design was chosen to satisfy several competing design considerations. First, we wanted to use identical timing parameters for both the MEG and fMRI. Second, we wanted large numbers of relatively short trials so that we could examine the temporal characteristics of the MEG signal, and third, we wanted long enough block lengths to allow the BOLD response to occur and recover.

MRI/fMRI Acquisition and Analysis

MRI data were acquired on a 3 T General Electric HDx scanner with an eight channel receive only head RF coil (Medical Devices). fMRI data were acquired using a gradient echo EPI sequence taking 37 axial slices of the whole brain at 3 mm isotropic voxel resolution with a 64×64 matrix size, echo time of 35 ms, 90° flip angle, and a TR of 2.5 s. For each participant, a 3D FSPGR scan with 1 mm isotropic voxel resolution was also obtained. Both MEG and fMRI data were co-registered to this high resolution structural scan.

Analysis of fMRI data was performed using the FSL software library (www.fmrib.ox.ac.uk/fsl). The following pre-processing was applied; motion correction using MCFLIRT [Jenkinson et al., 2002]; non-brain removal using Brain Extraction Tool (BET) [Smith, 2002]; spatial smoothing using a Gaussian kernel of FWHM 5 mm; mean-based intensity normalisation (grand mean scaling) of all volumes by the same factor and high-pass temporal filtering (Gaussian-weighted least-squares straight line fitting, with sigma = 50 s). For each 10 min run, the GLM was used to model each of the 10 conditions using a 5 s on/10 s off boxcar to describe each stimulus. This boxcar function was convolved with a standard HRF to account for haemodynamic effects. To combine the two runs for each individual, a second-level analysis was performed using a fixed effects model, by forcing the random effects variance to zero in FLAME (FMRIBs Local Analysis of Mixed Effects [Beckmann et al., 2003; Woolrich et al., 2004]). To assess the overall strength and location of the BOLD response in each participant and experiment, we created a mean condition combining all conditions in a fixed effects analysis in FLAME. The resultant z images were thresholded using Gaussian random field theory with a corrected significance threshold of $P < 0.05$ [Worsley et al., 1992].

MEG Acquisition and Analysis

Whole head MEG recordings were made using a CTF-Omega 275-channel radial gradiometer system sampled at 600 Hz. An additional 29 reference channels were recorded for noise cancellation purposes and the primary sensors were analysed as synthetic third-order gradiometers [Vrba and Robinson, 2001]. Three of the 275 channels were turned off because of excessive sensor noise. At the commencement of each active period of stimulation, a TTL pulse was sent to the MEG system. The location of three fiduciary markers (nasion, left and right preauricular) was monitored continuously through the MEG acquisition at a frequency of 10 Hz. In the event that participants moved more than 5 mm from their initial position, the experiment was paused between trials, and participants were asked by the experimenter to adjust their head position until it was less than 5 mm from the original position as detected by the MEG system and then the experiment continued.

After the experiment, each dataset was band-pass filtered using a fourth-order bi-directional IIR Butterworth filter into four frequency bands 0–20 Hz, 20–40 Hz, 40–60 Hz, and 60–80 Hz. Evenly spaced frequency bands were used so that the accuracy of covariance matrix estimation would be equal for each frequency band [Brookes et al., 2008]. This analysis revealed the bulk of activity in primary visual cortex occurred in the 40–60 Hz band. In later analyses, we also analysed broader gamma frequency bands of 40–80 Hz, 40–100 Hz, 20–80 Hz, and 20–100 Hz. The synthetic aperture magnetometry (SAM) beamformer algorithm [Robinson and Vrba, 1999] was used to create differential images of source power (pseudo-T statistics) for 5 s of baseline (−5 to 0 s) compared to 5 s of visual stimulation (0–5 s). Only 5 s of the baseline period was used for baseline estimation to achieve balanced covariance estimation between stimulated and un-stimulated states. Details of the calculation of SAM pseudo-T source image statistics are described in detail in a number of sources [Cheyne et al., 2003; Hillebrand et al., 2005; Robinson and Vrba, 1999; Singh et al., 2003; Vrba and Robinson, 2001]. To achieve MRI/MEG co-registration, prior to the MEG acquisition, fiduciary markers were placed at fixed distances from anatomical landmarks identifiable in participants' anatomical MRIs (tragus, eye centre). Fiduciary locations were verified afterwards using high-resolution digital photographs. For source localization, a multiple local-spheres [Huang et al., 1999] forward model was derived by fitting spheres to the brain surface extracted by FSLs BET. Estimates of the three-dimensional distribution of source power were derived for the whole head at 3-mm isotropic voxel resolution for each subject, frequency-band, and condition.

To assess the strength and localisation of gamma-band activity (40–60 Hz) in each participant, we computed a SAM image for all conditions versus the pre-stimulus baseline. To determine the significance of these images, we used permutation testing. In this approach, we randomly permuted the labelling of active and control data and generated new covariance matrices and SAM images for the permuted data [Cheyne et al., 2003]. Each SAM image was then recomputed 1000 times. To statistically threshold and correct the original SAM image for multiple comparisons, the omnibus test statistic obtained from the permutation distribution [Nichols and Holmes, 2002] was used ($P < 0.05$).

Virtual sensors were generated by using SAM beamformer coefficients obtained using the individual condition covariance matrices band pass filtered between 0 and 100 Hz and returning time-series from peak locations in

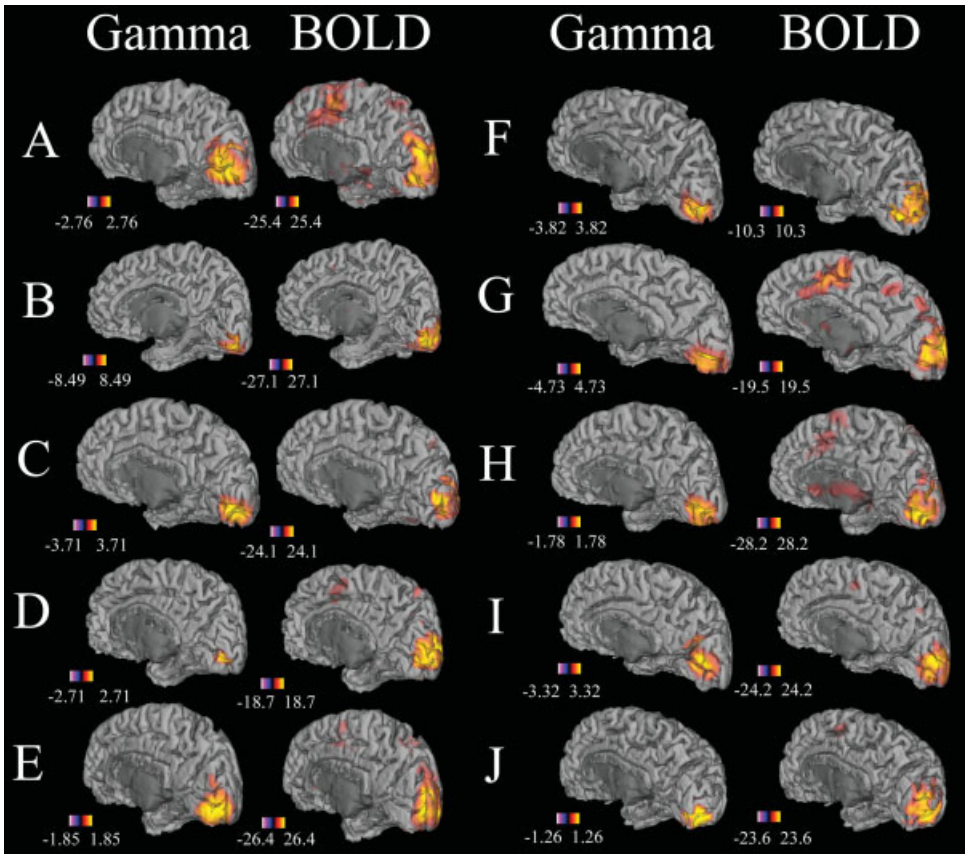

Figure 1.
The location of significant gamma-band and BOLD responses for all participants (**A**–**J**) for Experiment A overlaid onto semi-inflated right hemisphere cortical mesh models from those participants generated by FreeSurfer [Dale et al., 1999; Fischl et al., 1999]. Units for gamma rhythm are Pseudo-*T* values and *Z*-scores for BOLD. Both modalities are thresholded at $P < 0.05$, corrected for multiple comparisons. Similar images for all participants for Experiment B are included in the Supplemental Material. [Color figure can be viewed in the online issue, which is available at www.interscience.wiley.com.]

primary visual cortex for each trial [Robinson and Vrba, 1999]. Time frequency analysis of virtual sensors was conducted using the Hilbert transform. Time-frequency spectrograms are presented as a percentage change from the baseline energy for each frequency band.

Statistical Analysis of Condition Effects and Visualisation

To visualise the location of both BOLD and gamma-band sources, we constructed cortical mesh-models for each of our participants from their anatomical FSPGR scan using FreeSurfer [Dale et al., 1999; Fischl et al., 1999] (http://surfer.nmr.mgh.harvard.edu/). Functional scans were overlaid onto these mesh-models and the cortex partially inflated to allow visualisation of activation within sulci (for example, the calcarine sulcus) using the visualisation software mri3dX (https://cubric.psych.cf.ac.uk/Documentation/mri3dX/).

To assess the statistical significance of the different conditions, we extracted the peak amplitude value of the MEG and BOLD responses in primary visual cortex for each condition and participant. The normality of these data was first assessed using Kolmogorov-Smirnov tests. Data for each modality and subject was then subjected to a two-way repeated measures analysis of variance with factors of contrast (100%, 30%) and spatial frequency (3 cpd, 0.5 cpd) for Experiment A and stimulus type (square/sine) and spatial frequency (3 cpd, 0.5 cpd) for Experiment B.

RESULTS

Significant gamma band (40–60 Hz) and BOLD activity was detected in all 10 participants in each experiment when data were collapsed across the four conditions used in each experiment. Figure 1 illustrates gamma band and BOLD changes in all participants for Experiment A. In this figure, it can be seen that there is a high degree of spatial congruence between the two-imaging modalities with the sources of activation for most participants originating from the calcarine sulcus. Similar images for all 10 participants in Experiment B have been included in the Supplemental Material. For these analyses, the mean spatial separation between the peaks of the BOLD and gamma-band activity in each individual was 7 mm (range 4–11 mm).

For each experiment, trials were then partitioned by type and the amplitudes of the gamma-band response extracted for each condition. In Experiment A, participants were exposed to four stimulus types consisting of quadrant grating stimuli presented at two spatial frequencies (0.5 and 3 cpd) each at two contrast levels (100% and

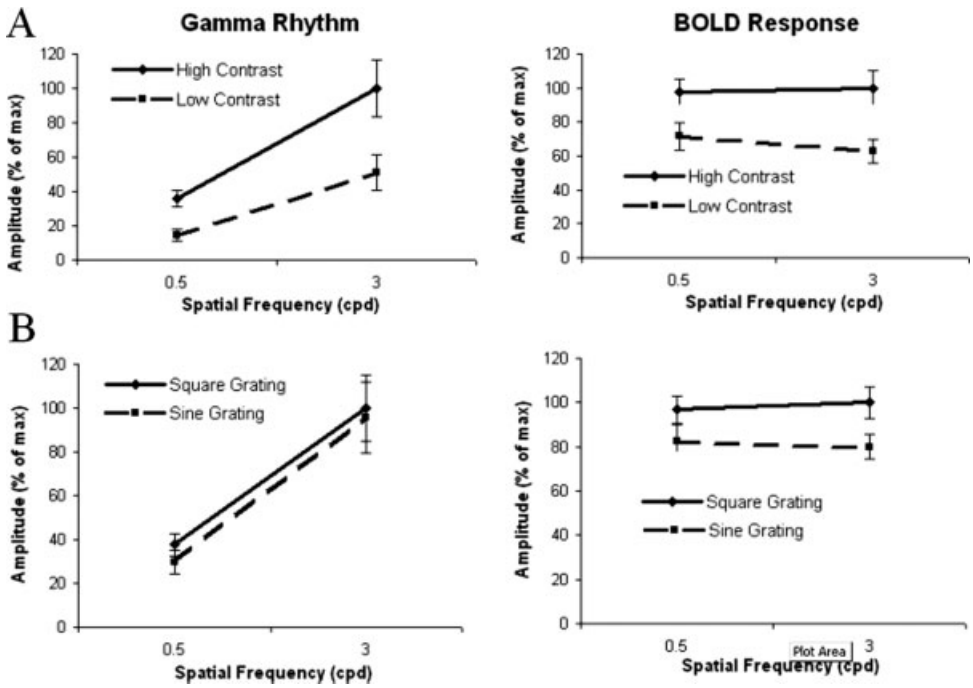

Figure 2.

A and **B**: Tuning curves of gamma-band and BOLD amplitudes in Experiment A and B, respectively. Data on the ordinate are expressed as a percentage of the maximum signal level for each dataset to facilitate comparison between the imaging modalities. In Experiment A, the high contrast stimulus was 100% and the low contrast 30%. Error bars represent ± s.e.m. Figure A demonstrates that both measures were sensitive to stimulus contrast but only the gamma rhythm was sensitive to spatial frequency. Figure B demonstrates that the BOLD response was not sensitive to spatial frequency but was to grating type, whereas the gamma rhythm was sensitive to spatial frequency and to a small extent grating type.

30%). In Experiment A, the gamma rhythm (40–60 Hz) data showed a significant main effect of spatial frequency ($F_{1,9}$ = 18.5, $P < 0.002$), contrast ($F_{1,9}$ = 35.6, $P < 0.001$), and an interaction effect ($F_{1,9}$ = 9.917, $P < 0.012$), whereas the BOLD response showed a main effect of contrast ($F_{1,9}$ = 47.97, $P < 0.001$), an interaction effect ($F_{1,9}$ = 6.83, $P < 0.028$) but no effect of spatial frequency ($F_{1,9}$ = 0.89). The amplitudes and standard errors of these effects for both experiments are presented in Figure 2A. These graphs clearly demonstrate the elevated response of both modalities to increased stimulus contrast and that only the gamma-band response increased in amplitude with spatial frequency.

In Experiment B, participants were exposed to four stimuli consisting of quadrant grating stimuli presented at two spatial frequencies (0.5 and 3 cpd) as either sine or square wave stimuli. In this experiment, the gamma rhythm data showed a significant main effect of spatial frequency ($F_{1,9}$ = 24.4, $P < 0.001$) and stimulus type ($F_{1,9}$ = 5.3, $P < 0.05$), whereas the BOLD data showed a main effect of type ($F_{1,9}$ = 103.8, $P < 0.001$) but not spatial frequency ($F_{1,9}$ = 0.9). The amplitudes and standard errors of these effects for both experiments are presented in Figure 2B. These graphs demonstrate that both modalities showed increased activity to square over sine wave stimuli, albeit smaller for the gamma-band response, and again that only the gamma-band response increased in amplitude with spatial frequency.

Although the strongest gamma-band activity (as measured by Pseudo-*T* scores) was found in the 40–60 Hz range, we obtained a similar pattern of statistical results when broader frequency bands were used, for example, 20–100 Hz. Results of these more extended statistical analyses are presented in Supplemental Tables. These results demonstrate that our findings are not a consequence of selection of a narrow frequency range to define the gamma band. No consistent desynchronisations were seen in primary visual cortex in lower frequency bands such as the alpha (~10 Hz) band even when examined with a more tightly focussed frequency band (5–15 Hz). Time-frequency analyses of virtual sensors from primary visual cortex were generated for each condition and participant. The grand averages of these results across participants are presented in Figure 3. In experimental conditions where a strong gamma-band response is present it can be seen that the gamma-band response is maintained for the duration of the stimulus presentation (0–5 s).

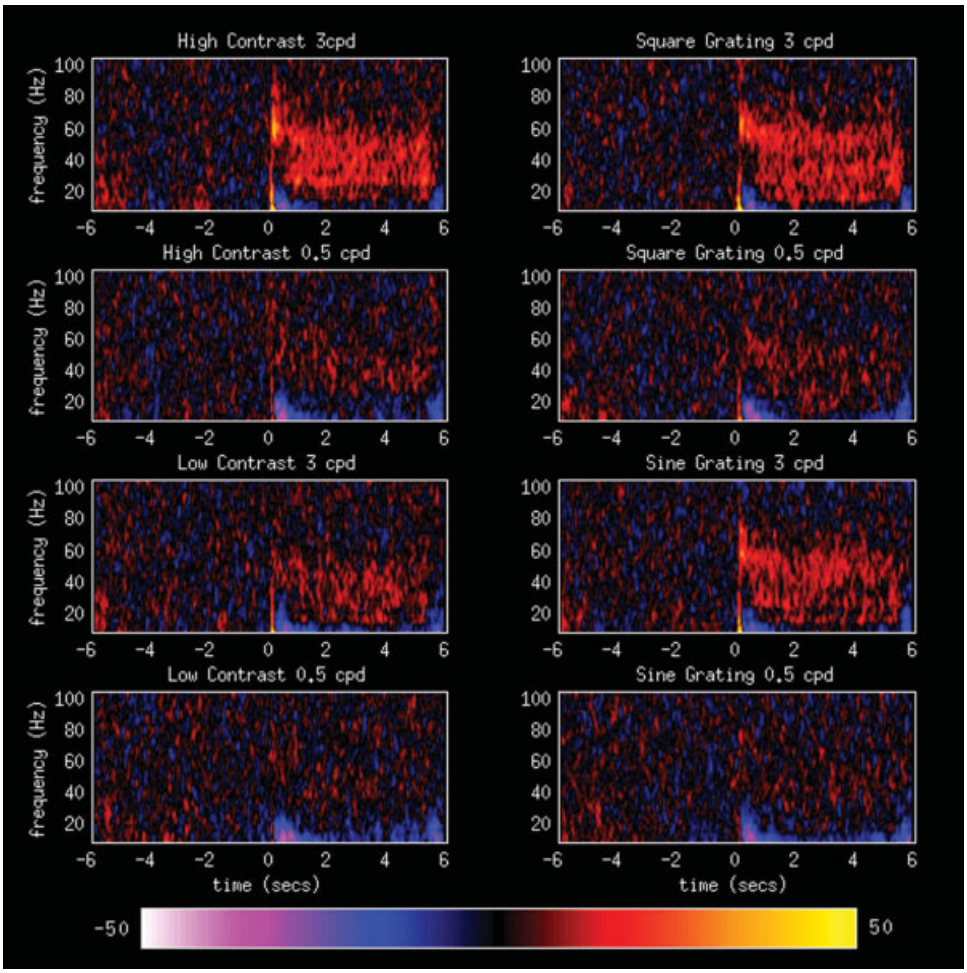

Figure 3.
Grand-averaged time-frequency spectrograms from MEG virtual sensors constructed in peak locations in primary visual cortex. Virtual sensors were generated from the peak gamma-band location in primary visual cortex for each condition. Energy values are represented as a percentage change from the baseline energy. The sustained nature of gamma-band activity during visual stimulation (0–5 s) can be seen in these spectrograms. [Color figure can be viewed in the online issue, which is available at www.interscience.wiley.com.]

DISCUSSION

In this experiment, we measured BOLD and gamma-band amplitudes while participants were stimulated with 0.5 and 3 cpd grating stimuli at either high and low contrast levels or as square and sine waves. It was found that gamma-band amplitudes showed a ~300% increase in amplitude with stimulus spatial frequency while the BOLD response was insensitive to spatial frequency. This pattern was found regardless of stimulus contrast or stimulus type. Here, we used the dense sensor coverage afforded by MEG to confirm that gamma-band and BOLD effects were emanating from the same cortical area, namely primary visual cortex. The mean spatial separation between the peaks of the BOLD and gamma-band activity in each individual was 7 mm (range 4–11 mm) consistent with previous work by ourselves [Muthukumaraswamy and Singh, 2008] and others [Brookes et al., 2005; Moradi et al., 2003]. This error can easily be accounted for by movement of participants during scanning sessions or co-registration errors between the two imaging modalities across scanning sessions [Singh et al., 1997] (more extensive discussion of this topic can be found in [Muthukumaraswamy and Singh, 2008] and [Brookes et al., 2005]). Given that the Pythagorean distance across a functional voxel in this study was 5.2 mm it suggests that the spatial localisation error was as little as 1–2 functional voxels.

As with our previous experiment [Muthukumaraswamy and Singh, 2008], where we compared spatiotemporal frequency tuning between BOLD and gamma-band responses, we again found a large discrepancy between BOLD and gamma-band amplitudes to the two spatial frequencies used. In both experiments, we found in primary visual cortex that gamma-band amplitudes were three times larger for a 0.5 cpd stimulus compared to a 3 cpd stimulus, whereas, the BOLD response for these stimuli showed a similar amplitude. In the previous experiment using 100% contrast stimuli, the flat BOLD response may have been due to either a ceiling effect or a contrast saturation effect. To address this issue here in Experiment A, we used both maximal contrast (100%) and a lower contrast level (30%) and demonstrate that the differential effect of spatial frequency occurs also at lower contrast levels, that is, it is not a ceiling effect. The main effects of

increasing stimulus contrast are an increase in the amplitudes of both gamma-band oscillations and the BOLD response (Fig. 2A) and are entirely consistent with previous work in both humans [Hall et al., 2005] and animals [Logothetis et al., 2001; Niessing et al., 2005].

In our previous experiment [Muthukumaraswamy and Singh, 2008] square wave grating stimuli were used. Square wave stimuli contain harmonic spatial frequencies and if the BOLD response was differentially sensitive to these harmonics this may have elevated the BOLD response in one condition, flattening the spatial frequency response. In the current study, the similar response to spatial frequency for both sine and square wave stimuli suggests that the differential effect of spatial frequency is not caused by harmonic spatial frequencies within the stimulus set. Taken together the current experiments strongly suggest that BOLD and gamma-band amplitudes can be functionally decoupled; a result that implies, at least for primary visual cortex, that increased amplitude of gamma-band oscillations is not sufficient to drive the subsequent BOLD response. These results are consistent with previous work on spatial frequency tuning in primary visual cortex, which shows relatively flat tuning curves for BOLD [Singh et al., 2000] but curves for gamma which peak at 3 cpd [Adjamian et al., 2004]. Our data also suggest that gamma oscillation amplitudes only display a slight increase of activity for square over sine wave stimuli suggesting that sharp edges are not critical for the generation of gamma oscillations in primary visual cortex [Gray et al., 1989; Gray and Singer, 1989] when using surface recording techniques such as MEG or EEG.

Although in this experiment we have focussed on gamma-band power changes in primary visual cortex, it should be pointed out that it has been found in other cortical areas and paradigms that decreases in oscillatory power in lower frequency bands have also be shown to overlap with the BOLD response. Singh et al. [2002] found in a covert letter fluency task that the BOLD response in left hemisphere language areas overlapped with alpha and beta band power decreases and in a biological motion discrimination task that BOLD overlapped with alpha/beta power decreases in occipital cortex. In a basic visual stimulation paradigm, Brookes et al. [2005] found in visual cortex that alpha band power decreases also co-localised with BOLD and gamma power increases. In the current experiment, alpha-band responses were found to be somewhat variable even when examined with a relatively focussed frequency band (5–15 Hz). Brookes et al. also comment that the alpha band changes display a greater degree of variability than the gamma-band responses and this is consistent with the data here. In Figure 3, alpha band power decreases can be seen to occur to both stimulus onset and offset but often the peaks of alpha power decreases in individuals were located in extrastriate areas so that these effects may reflect beamformer 'bleed' from adjacent cortical areas. In another direct comparison of oscillatory MEG responses and BOLD in a two choice reaction time task, Winterer et al. [2007] found that positive BOLD responses can be accompanied by ERD/ERS complexes in the same cortical area and that this spatial co-localisation can occur across relatively broad frequency ranges that vary across cortical locations. Taken together, all these data suggest no simple model of how BOLD changes co-localise with oscillatory changes—rather they suggest that the cerebral cortex is non-homogenous with respect to how its oscillatory responses may potentially correlate with the BOLD response. The current data go further and demonstrate that spatial co-localisation need not imply functional similarity when stimulus parameters are experimentally manipulated.

The results in these experiments suggest that the amplitude of the BOLD response in primary visual cortex cannot be fully explained by increases in local gamma-band synchronisation. This empirical result is predicted by previous modelling work, which demonstrates that it would require only 1% of mini-columns in an area acting synchronously to account for 75% of the measured EEG/MEG scalp signals [Nunez, 1981]. Changes in stimulus parameters, such as spatial frequency, might generate significant variation in the degree of cross-columnar gamma synchronisation. However, as the population of neurons acting synchronously is only a small proportion of the total neuronal population, this variation may not be reflected in the BOLD response, which integrates across both synchronous and asynchronous populations [Nunez and Silberstein, 2000]. This result has important consequences for the interpretation of functional imaging results in general as it demonstrates that the two imaging modalities can be differentially sensitive to stimulus-related aspects of neuronal activity. Specifically, our data demonstrates that experimental effects may be present in oscillatory MEG data that are absent in the BOLD response.

REFERENCES

Adjamian P, Holliday IE, Barnes GR, Hillebrand A, Hadjipapas A, Singh KD (2004): Induced visual illusions and gamma oscillations in human primary visual cortex. Eur J Neurosci 20:587–592.

Beckmann CF, Jenkinson M, Smith SM (2003): General multilevel linear modeling for group analysis in FMRI. Neuroimage 20:1052–1063.

Brookes MJ, Gibson AM, Hall SD, Furlong PL, Barnes GR, Hillebrand A, Singh KD, Holliday IE, Francis ST, Morris PG (2005): GLM-beamformer method demonstrates stationary field, alpha ERD and gamma ERS co-localisation with fMRI BOLD response in visual cortex. Neuroimage 26:302–308.

Brookes MJ, Vrba J, Robinson SE, Stevenson CM, Peters AM, Barnes GR, Hillebrand A, Morris PG (2008). Optimising experimental design for MEG beamformer imaging. Neuroimage 39:1788–1802.

Cheyne D, Gaetz W, Garnero L, Lachaux J-P, Ducorps A, Schwartz D, Varela FJ (2003): Neuromagnetic imaging of cortical oscillations accompanying tactile stimulation. Cogn Brain Res 17:599–611.

Dale AM, Fischl B, Sereno MI (1999): Cortical surface-based analysis. I. Segmentation and surface reconstruction. Neuroimage 9:179–194.

Fischl B, Sereno MI, Dale AM (1999): Cortical surface-based analysis. II. Inflation, flattening, and a surface-based coordinate system. Neuroimage 9:195–207.

Gray CM, Konig P, Engel AK, Singer W (1989): Oscillatory responses in cat visual-cortex exhibit inter-columnar synchronization which reflects global stimulus properties. Nature 338: 334–337.

Gray CM, Singer W (1989): Stimulus-specific neuronal oscillations in orientation columns of cat visual-cortex. Proc Natl Acad Sci USA 86:1698–1702.

Hall SD, Holliday IE, Hillebrand A, Singh KD, Furlong PL, Hadjipapas A, Barnes GR (2005): The missing link: Analogous human and primate cortical gamma oscillations. Neuroimage 26:13–17.

Hillebrand A, Singh KD, Holliday I, Furlong PL, Barnes GR (2005): A new approach to neuroimaging with magnetoencephalography. Hum Brain Mapp 25:199–211.

Huang MX, Mosher JC, Leahy RM (1999): A sensor-weighted overlapping-sphere head model and exhaustive head model comparison for MEG. Phys Med Biol 44:423–440.

Jenkinson M, Bannister P, Brady M, Smith S (2002): Improved optimization for the robust and accurate linear registration and motion correction of brain images. Neuroimage 17:825–841.

Kayser C, Kim M, Ugurbil K, Kim DS, Konig P (2004): A comparison of hemodynamic and neural responses in cat visual cortex using complex stimuli. Cereb Cortex 14:881–891.

Logothetis NK, Pauls J, Augath M, Trinath T, Oeltermann A (2001): Neurophysiological investigation of the basis of the fMRI signal. Nature 412:150–157.

Moradi F, Liu LC, Cheng K, Waggoner RA, Tanaka K, Ioannides AA (2003): Consistent and precise localization of brain activity in human primary visual cortex by MEG and fMRI. Neuroimage 18:595–609.

Muthukumaraswamy SD, Singh KD (2008): Spatiotemporal frequency tuning of BOLD and Gamma band MEG responses compared in primary visual cortex. Neuroimage 40:1552–1560.

Nichols TE, Holmes AP (2002): Nonparametric permutation tests for functional neuroimaging: A primer with examples. Human Brain Mapping 15:1–25.

Niessing J, Ebisch B, Schmidt KE, Niessing M, Singer W, Galuske RAW (2005): Hemodynamic signals correlate tightly with synchronized gamma oscillations. Science 309:948–951.

Nir Y, Fisch L, Mukamel R, Gelbard-Sagiv H, Arieli A, Fried I, Malach R (2007): Coupling between neuronal firing rate, gamma LFP, and BOLD fMRI is related to interneuronal correlations. Curr Biol 17:1275–1285.

Nunez PL.1981. Electric Fields of the Brain: The Neurophysics of EEG. New York: Oxford University Press.

Nunez PL, Silberstein RB (2000): On the relationship of synaptic activity to macroscopic measurements: Does co-registration of EEG with fMRI make sense? Brain Topogr 13:79–96.

Parkes LM, Bastiaansen MCM, Norris DG (2006): Combining EEG and fMRI to investigate the post-movement beta rebound. Neuroimage 29:685–696.

Robinson SE, Vrba J (1999): Functional neuroimaging by synthetic aperture manetometry (SAM). In: Yoshimoto T, Kotani M, Kuriki S, Karibe H, Nakasato N, editors. Recent Advances in Biomagnetism. Sendai: Tohoku University Press. pp 302–305.

Singh KD, Barnes GR, Hillebrand A (2003): Group imaging of task-related changes in cortical synchronisation using nonparametric permutation testing. Neuroimage 19:1589–1601.

Singh KD, Holliday IE, Furlong PL, Harding GFA (1997): Evaluation of MRI-MEG/EEG co-registration strategies using Monte Carlo simulation. Electroencephalogr Clin Neurophysiol 102:81–85.

Singh KD, Smith AT, Greenlee MW (2000): Spatiotemporal frequency and direction sensitivities of human visual areas measured using fMRI. Neuroimage 12:550–564.

Smith SM (2002): Fast robust automated brain extraction. Hum Brain Mapp 17(3):143–155.

Vrba J, Robinson SE (2001): Signal processing in magnetoencephalography. Methods 25:249–271.

Winterer G, Carver FW, Musso F, Mattay V, Weinberger DR, Coppola R (2007): Complex relationship between BOLD signal and synchronization/desynchronization of human brain MEG oscillations. Hum Brain Mapp 28:805–816.

Woolrich MW, Behrens TEJ, Beckmann CF, Jenkinson M, Smith SM (2004): Multilevel linear modelling for FMRI group analysis using Bayesian inference. Neuroimage 21:1732–1747.

Worsley KJ, Evans AC, Marrett S, Neelin P (1992): A 3-dimensional statistical-analysis for Cbf activation studies in human brain. J Cereb Blood Flow Metabol 12:900–918.